Low-temperature infrared absorption of *n*-type GaP

E. Goldys
Institute of Experimental Physics, Warsaw University, Hoza 69, 00-681 Warsaw, Poland

P. Galtier and G. Martinez
Service National des Champs Intenses, Centre National de la Recherche Scientifique, BP 166 X, 38042 Grenoble Cédex, France

I. Gorczyca
High Pressure Research Center, Polish Academy of Sciences, 01142 Warsaw, Poland
(Received 5 February 1987)

Detailed measurements of the low-temperature infrared absorption of tellurium- and sulfur-doped *n*-type gallium phosphide have been performed. The set of well-characterized samples with neutral-donor concentrations ranging from 1.5×10^{17} to 6.4×10^{18} cm^{-3} allowed us to follow the concentration dependence of the observed absorption band. The spectra have been described quantitatively, including the absolute value of the absorption coefficient. The contributions of transitions from the donor ground state to the different final states have been separated. No effect of the clustering of donors has been observed on the photoionization part of the absorption. The line-shape of the transition to the resonant state has been deduced. Its width and its energy position are analyzed in terms of Fano-type interaction with the X_1-band continuum.

I. INTRODUCTION

This paper is concerned with the experimental study of the near-infrared absorption band in *n*-type GaP at low temperatures. It has been established[1–3] that this absorption band involves electron transitions from the donor ground state to several different states above the bottom of the conduction band. The electronic structure in the region above the minimum of the conduction band is now fairly well known.[4] It shows some similarity to the structure of bands in Si. The conduction band in Si is doubly degenerate at the X point of the Brillouin zone. The antisymmetric crystal potential in GaP removes this degeneracy. The two resulting split bands have a symmetry which depends on the choice of the origin.[5] When it is chosen on the P site, as it will be in this paper, the lower band at the X point has X_1 symmetry and the higher one X_3 symmetry. The energy difference δ between the bands at X is around 0.3 eV.[2] As a result of the interaction, the bands are nonparabolic. The X_1 band has a "camel-back" shape with two minima along the Γ-X axis located at $0.08(2\pi/a_0)$ from the X point, where a_0 is the GaP lattice constant. The minimum of the X_3 band is at the X point. The ground state of a P-site donor lies about 0.1 eV below the minimum of the X_1 band. There is also a resonant donor state under the minimum of X_3. Such a structure allows for several absorption processes in the range 0.25–1.4 eV. A schematic representation of the possible optical transitions at 77 K is shown in Fig. 1. All these absorption processes overlap, giving rise to a broad and structured band. The experimental cross sections of this absorption band reported so far present some discrepancies. The cross section demonstrated by Onton[3] in the region corresponding to process (b) in Fig. 1 for Te-doped samples is significantly higher than the one shown by Pikhtin and Yaskov.[2]

Until now there was no attempt to obtain a coherent picture of all the absorption processes based on actual knowledge of the band and donor parameters, which are determined quite precisely now.[6–9] In the most systematic study, Pikhtin and Yaskov[2] calculated the absorption assuming the X_3 band to be spherical and parabolic, and the donor ground state as spherical and hydrogenic. The agreement of this model with the experimental data is not satisfactory (the effective-mass ratio thus obtained, $m^*_{X_3}/m^*_{X_1}=0.2$, cannot be easily explained).

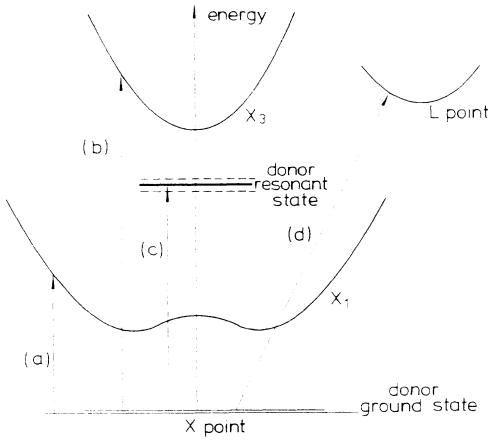

FIG. 1. Schematic diagram of the possible optical transitions at low temperatures in the 0.3–1.4-eV energy range for *n*-type GaP.

One of the motivations for this work was to check if the complex electronic structure of the band and the donor is reflected in the infrared absorption at 77 K. We tried also to get more insight into the properties of the resonant state.

Study of electron paramagnetic resonance (EPR) of shallow donors in GaP and of Raman scattering of bound phonons[10] demonstrates that, in the range of concentrations studied, the effect of the donor clustering can be seen. It was our aim to examine if any clustering effects would manifest themselves in the infrared absorption.

II. EXPERIMENTAL PROCEDURE

The samples used were cut and mechanically polished from GaP:S and GaP:Te ingots doped during growth. Several methods have been used to determine the neutral-donor concentration, a factor which is fundamental for the magnitude of the absorption cross section. Spark-source mass spectroscopy (SSMS) measurements have been performed on some samples. The concentration of sulfur or tellurium atoms which were the major dopants is thus obtained, as well as the concentrations of residual impurities: carbon, oxygen, and others. From these measurements, the determination of the neutral-donor concentrations may not be very accurate. In addition, we performed Hall-effect measurements at 300 K which give the free-electron concentration. The same quantity has been deduced from plasmon energy measurement at 300 K. Assuming a small compensation and one type of donor, the neutral-donor concentration (N_D) can be deduced. The concentrations for each sample obtained by these methods (see Table I) show some differences. The values of N_D we have chosen (last column in Table I) are those which seem the most reliable to us. In any case these values have to be accepted with an error of $\pm 30\%$. The samples used in this experiment were the same as in the work[10] of Galtier *et al.*

The absorption coefficient (α) of these samples was measured in the range 0.25–1.4 eV. In order to provide an efficient cooling of the samples they were compressed between two thin sapphire plates mounted on the cold finger of the cryostat. We did not observe any changes of the spectrum during the time of experiment, which indicates that the temperature $\simeq 80$ K has been obtained. Light was analyzed with a grating spectrometer under vacuum conditions and detected by a cooled InSb detector (with a cutoff $\simeq 0.25$ eV).

The sample thicknesses were in the range 10–500 μm. For some of the thinnest samples there were traces of interference effects on the transmission spectra; these samples were rejected. All transmission curves were measured using the in-out method. The absorption coefficient has been calculated using the value of refractive index $n = 3.0$ in the whole region examined.[11] The measured absorption curves for all samples are shown in Fig. 2.

III. THEORETICAL MODEL

The interpretation of the observed spectra requires accurate information about all the absorption processes, (a), (b), (c), and (d) (Fig. 1). Knowledge of the shape of the conduction bands and of the wave function of the donor ground state is necessary.

As has been stated,[4,12,13] the conduction band of GaP is strongly nonparabolic. There are several nonparabolic terms in the dispersion equation. We keep only the most important one, which is responsible for the "camel back." We assume the origin for the wave vector to be at the X point of the Brillouin zone. The dispersion relation is then

$$E_{X_1(X_3)}(\mathbf{k}) = \frac{\hbar^2}{2m_\perp}(k_x^2+k_y^2)+\frac{\hbar^2}{2m_\parallel}k_z^2 \pm \left[\left[\frac{\hbar}{m}\right]^2 k_z^2 p_z^2 + \left[\frac{\delta}{2}\right]^2\right]^{1/2}, \quad (1)$$

where the subscript X_1 (X_3) corresponds to the X_1 (X_3) band, $m_\parallel$ and $m_\perp$ are the effective-mass parameters,[12] m is the free-electron mass, and $\mathbf{p}$, the momentum matrix element between the X_1 and X_3 wave functions, has only one nonzero component p_z.

Such a band structure influences the wave function of a shallow donor. An additional source of complication is a large intervalley-scattering and central-cell correction which causes deviations from the simple effective-mass theory. The exact wave function is not known and use of the variational technique is required to evaluate it.[14]

For our purpose we have chosen a simple model wave function which reflects the camel-back shape of the conduction band and the anisotropy of the effective mass. It will allow us to determine the extension of the donor wave function in directions parallel and perpendicular to the valley. This wave function can be formally written as

TABLE I. The neutral-donor concentrations of sulfur-doped GaP (S) and tellurium-doped GaP (T) samples measured by different techniques. Last column gives our choice for N_D.

Sample number	Coupled LO-phonon–plasmon Raman scattering (cm^{-3})	Hall effect (cm^{-3})	SSMS (cm^{-3})	N_D (cm^{-3})
S_1	3.7×10^{17}	4.4×10^{17}	3.9×10^{17}	4.0×10^{17}
S_4	1.1×10^{18}	1.2×10^{18}		1.2×10^{18}
S_6	4.8×10^{18}			4.8×10^{18}
S_7	6.6×10^{18}	6.4×10^{18}	5.8×10^{18}	6.4×10^{18}
T_1	1.5×10^{17}	2×10^{17}		1.5×10^{17}
T_5	8.9×10^{17}	8×10^{17}		8.9×10^{17}

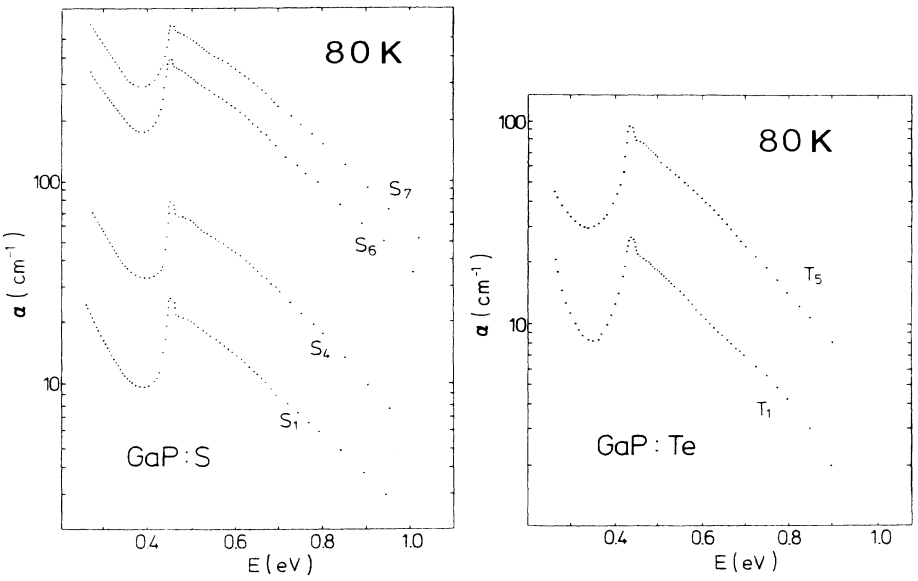

FIG. 2. Experimental absorption coefficient for n-type GaP samples.

$$\psi_1(\mathbf{r})=\psi_{X_1}(\mathbf{k}_X,\mathbf{r})F_1^0(\mathbf{r}) ,$$

where

$$F_1^0(\mathbf{r})=A\exp\left\{-\left[\left[\frac{x}{a}\right]^2+\left[\frac{y}{a}\right]^2+\left[\frac{z}{b}\right]^2\right]^{1/2}\right\}$$

$$\times[\exp(i\mathbf{k}_0\cdot\mathbf{r})+\exp(-i\mathbf{k}_0\cdot\mathbf{r})] , \quad (2)$$

$\psi_{X_1}(\mathbf{k}_X,\mathbf{r})$ is an X_1 Bloch function at the X point, k_0 is the position of the minimum of the X_1 band on a and b are the Bohr radii in the directions perpendicular and parallel to z, and A is the normalization constant.

The absorption process (a) has been studied previously by Kopylov and Pikhtin.[12] The authors have shown that the matrix element governing the transition between the donor ground state and the X_1 band is a linear function of k only near the X point and quickly reaches a constant value. Subsequently the absorption coefficient of process (a) has an energy dependence given by

$$\alpha_{(a)}\sim\frac{(\hbar\omega-E_I)^{1/2}}{(\hbar\omega)^3} , \quad (3)$$

where E_I is the ionization energy of the impurity. The experimental data presented in Ref. 12 follow this dependence.

The Fermi golden rule[15] allows us to calculate the absorption coefficient for process (b):

$$\alpha_{(b)}(\hbar\omega)=\frac{4\pi^2}{ne\omega}\left[\frac{e}{m}\right]^2$$

$$\times\sum_i\int\frac{2d^3k}{(2\pi)^3}|\epsilon\cdot\mathbf{M}_{if}|^2$$

$$\times\delta(E_{X_3}(\mathbf{k})-\delta/2-E_I-\hbar\omega) , \quad (4)$$

where c is the velocity of light, i numbers the different impurities, ϵ is the polarization vector of the incident radiation, $\mathbf{M}_{if}$ is the momentum matrix element between the impurity wave function and the X_3 wave function (2), and e is the electron charge. We obtain the following expression for the absorption coefficient of process (b):

$$\alpha_{(b)}(\hbar\omega)=N_D\frac{\omega}{nc}\frac{4\pi^2}{\omega^2}\left[\frac{e}{m}\right]^2\frac{1}{3}p_z^2 32\frac{a^2b}{\pi}\frac{1}{1+(1+bx_0^2)^{-2}}\sqrt{\delta}\frac{m_\perp^2 m_\parallel}{\hbar^3}$$

$$\times\int_0^{[\epsilon+p-(2p\epsilon+p^2+1)^{1/2}]^{1/2}}dx\left[\frac{1}{\{1+\alpha[\epsilon-x^2-(2px^2+1)^{1/2}]+\beta(x-x_0)^2\}^2}\right.$$

$$\left.+\frac{1}{\{1+\alpha[\epsilon-x^2-(2px^2+1)^{1/2}]+\beta(x+x_0)^2\}^2}\right]^2 , \quad (5)$$

where

$$\alpha=\frac{\delta}{2}\frac{1}{R_A}\frac{m_\perp}{m_A}\ ,\quad \beta=\frac{\delta}{2}\frac{1}{R_B}\frac{m_\parallel}{m_B}\ ,$$

$$R_A=\frac{e^4 m_A}{2\epsilon_D^2\hbar^2}\ ,\quad R_B=\frac{e^4 m_B}{2\epsilon_D^2\hbar^2}\ ,$$

$$m_A=\frac{\epsilon_D\hbar^2}{ae^2}\ ,\quad m_B\equiv\frac{\epsilon_D\hbar^2}{be^2}\ ,$$

$$\epsilon=\frac{2(\hbar\omega-\delta/2-E_I)}{\delta}\ ,\quad p=\frac{2p_z^2 m_\parallel}{m^2\delta}\ ,\quad x_0=\frac{\hbar\,|\,\mathbf{k}_0\,|}{(m_\parallel\delta)^{1/2}}\ .$$

ϵ_D is the static dielectric constant.

The absorption coefficient for the indirect transition (d) can be calculated in a similar way. We consider only the phonon emission process. The matrix element of the electron-phonon interaction is assumed to be constant. The only contribution taken into account for this process corresponds to a real transition of an electron to the X_3 band with the subsequent emission of a phonon and the transition of the electron to the L point. We obtain

$$\alpha_{(d)}(\hbar\omega)=N_D C^2\frac{\omega}{nc}\frac{4\pi^2}{\omega^2}\left[\frac{e}{m}\right]^2\tfrac{1}{3}p_z^2 \times\left|\int\frac{\tilde{F}_1^0(\mathbf{k})d^3k}{-\frac{\delta}{2}-E_I+\hbar\omega-E_{X_3}(\mathbf{k})}\right|^2 \times\rho_L(\hbar\omega-E_I-\delta-\delta_L)\ , \tag{6}$$

where $\tilde{F}_1^0(\mathbf{k})$ is a Fourier transform of $F_1^0(\mathbf{r})$, δ_L is the gap between the X_3 band and the first conduction band at the L point, and ρ_L is the density of states near the L minimum.

Finally, the calculation of the absorption coefficient for process (c) is performed by means of a Green's-function technique. The final state $|f\rangle$ in this transition is a result of the interaction between the localized state and the X_1-band continuum. The absorption coefficient from the ground state of a donor $|i\rangle$ to the state $|f\rangle$ can be expressed as

$$\alpha_{(c)}(\hbar\omega)\propto\sum_{i,f}|\langle i\,|\,\mathbf{p}\,|\,f\rangle|\,\delta(E_f-(E_I+\delta/2)-\hbar\omega) =\frac{1}{\pi}\mathrm{Im}\sum_i\langle i\,|\,\mathbf{p}\,|\,f\rangle\langle f\,|\,G\,|\,f\rangle\langle f\,|\,\mathbf{p}\,|\,i\rangle\ , \tag{7}$$

where G is the Green's function of the system including the interaction between the localized state and the continuum. G is diagonal in the $|f\rangle$ basis. Summation over repeated indices is implicit in (7). We choose a new basis composed of the localized state located under the X_3 minimum, which has a wave function $\phi_2^0(\mathbf{r})$, and the states of the X_1 band, $\psi_1(\mathbf{k},\mathbf{r})$, all unperturbed by the mutual interaction. We assume that the matrix element $\langle i\,|\,\mathbf{p}\,|\,\alpha\rangle$ for $\mathbf{k}$ values which correspond to an energy near the resonance is much smaller when $|\alpha\rangle$ describes the X_1 band than for the localized state. This approach is justified because the resonant energy is located a few hundred meV above the bottom of the X_1 band and the effective mass of the band is large. Therefore

$$\alpha_{(c)}(\hbar\omega)\propto\sum_i|\langle i\,|\,\mathbf{p}\,|\,\alpha_e\rangle|^2\langle\alpha_l\,|\,G\,|\,\alpha_e\rangle\ , \tag{8}$$

where $|\alpha_l\rangle$ stands for a localized state.

The unknown matrix element of the G function between the localized states is easy to calculate from the definition $(H-E)G=1$, H being the Hamiltonian of the system. The resulting absorption coefficient is

$$\alpha_{(c)}(\hbar\omega)=N_D\frac{\omega}{nc}\frac{4\pi^2}{\omega^2}\left[\frac{e}{m}\right]^2\frac{\hbar^2}{\pi}|\langle\psi_1(\mathbf{r})\,|\,\mathbf{p}\,|\,\phi_2^0(\mathbf{r})\rangle|^2 \times\frac{\Gamma(\hbar\omega)}{[E_2^0-\hbar\omega-R(\hbar\omega)]^2+[\Gamma(\hbar\omega)]^2}\ , \tag{9}$$

where E_2^0 is the position of the localized state without the interaction and

$$R(E)=\mathrm{P}\int d^3k\frac{|\,V(\mathbf{k})\,|^2}{E_{X_1}(\mathbf{k})-E}\ ,$$
$$\Gamma(E)=\int d^3k\,|\,V(\mathbf{k})\,|^2\delta(E_{X_1}(\mathbf{k})-E)\ . \tag{10}$$

P stands for the principal value and

$$V(\mathbf{k})=\int d^3r\,\psi_1(\mathbf{k},\mathbf{r})V(\mathbf{r})\phi_2^0(\mathbf{r}) \tag{11}$$

is the coupling term and $U(\mathbf{r})$ is the impurity potential. We will require this model to describe the absorption of all the samples with the same parameters for each donor species.

IV. THE APPLICATION OF THE MODEL

As is shown in Fig. 2, the typical absorption curve consists of a background which grows on the low-energy side [corresponding to (a)], and a structured band (b) + (c) + (d) which we want to study. In order to get more insight into the structure of this band it is necessary to separate it from the underlying absorption (a). The examination of the experimental curves shows that before the onset of the band the experimental points could be fitted by a law such as $A\lambda^\eta$ where A is a constant and η is around 3. We could therefore try to extrapolate it to the shorter-wavelength region, thus obtaining the contribution of (a) to the total absorption. In the range of 0.3–0.7 eV, the wavelength dependence of formula (3) and that of the phenomenological formula $A\lambda^\eta$ are roughly the same. The existing difference influences mainly the magnitude of the absorption (b) + (c) + (d) by a few percent but not its shape. We decided to subtract the absorption (a) according to the formula (3) of Kopylov. The error which arises, added to the uncertainty in the determination of the concentration, influences the value of the cross section mainly in a proportional way. The subtraction procedure in itself is a source of error. In the region 0.3–0.7 eV, where the band (b) + (c) + (d) begins, the absorption (a) is almost equal to the total absorption and is rather large in comparison to the rest of the absorption curve. Therefore

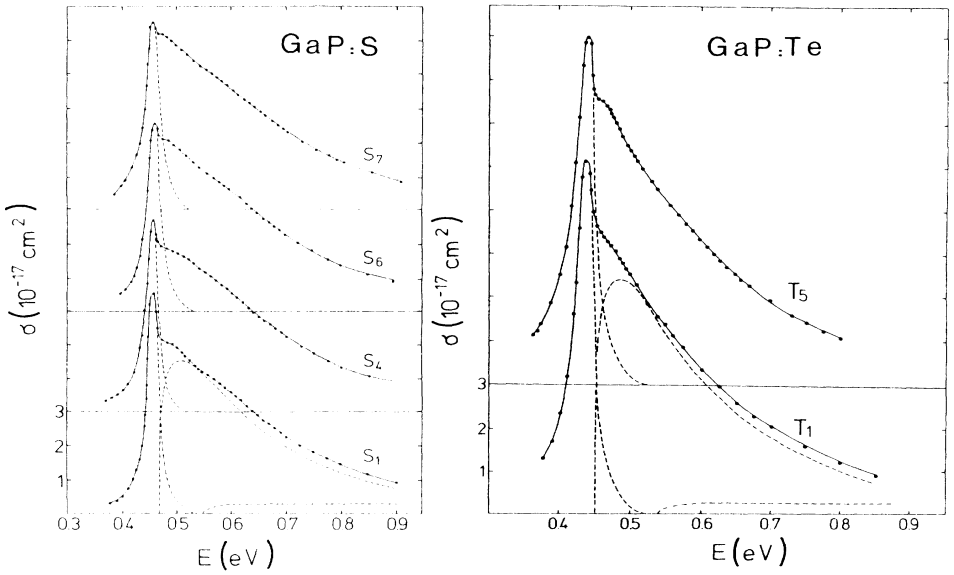

FIG. 3. The absorption band after subtraction of (a) transitions for GaP:S and GaP:Te. The dots are the experimental points. The dashed lines represent the calculated contributions of (b), (c), and (d) transitions, the solid line, the sum of all theoretical contributions. The curves for different samples are displaced vertically, the vertical scale is for S_1 (T_1) samples.

the result of the subtraction cannot reproduce very precisely the real onset of the (b) + (c) + (d) band. Moreover, any uncertainty of the fit of the formula (3) to the experimental points in the region 0.25–0.35 eV has a large influence on this onset too. It follows that after the subtraction procedure the error in the determination of the absorption is relatively larger in the range 0.3–0.4 eV than in the range 0.5–0.9 eV, where the total absorption is stronger and (a) weaker. Another region where the error in the measurement of the absorption coefficient increases is above 0.8–0.9 eV, where the total absorption decreases, so the experimental condition $\alpha d \approx 1$ is no longer fulfilled (d is the thickness of the sample).

The resulting band [(b) + (c) + (d) transitions] is shown in Fig. 3 (dots). The peak which is seen on all the spectra is due to process (c); the remaining part of the band corresponds to the photoionization-type process (b) + (d). The onset of (d) can be noticed after a detailed examination of the short wavelength shoulder of absorption (b). We did not attempt to fit the value of absorption (d) because the small relative magnitude of (d) with respect to (b) does not allow us to find an accurate value of the constant C in (6). We fitted only the energy dependence of the (d) absorption.

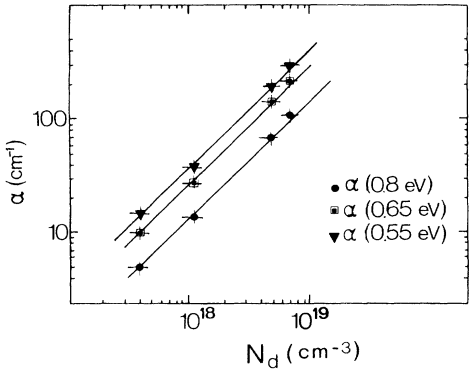

FIG. 4. The neutral-donor-concentration dependence of the absorption coefficient of the (b) + (c) + (d) band for different energies of light.

The whole photoionization part of the band appears to be proportional to the neutral-donor concentration (Fig. 4). Both the value and the shape of the absorption band can be properly described with a realistic set of parameters and the proposed model of Eq. (5). The parameters are given in Table II together with a comparison with other experimental and theoretical data. Therefore we are able to deduce the shape of the transition (c), which has never been shown explicitly, from the experimental absorption curve.

V. DISCUSSION OF THE RESULTS

A. Donor and band properties

As is shown in Table II, the agreement between the parameters used in this model and the published data is very good. The essential fitting parameters in our model were the perpendicular and parallel Bohr radii. Both the magnitude and the shape of the (b) + (d) part were quite sensitive to these quantities. The small change of the remaining parameters in the model, e.g., p_z, did not influence a and b very much. This allowed us to determine both these radii separately for S- and Te-doped samples. The ratio of Bohr radii ($b/a = 2.1$) agrees well with the one given by Chang and McGill in (Ref. 14).

The only nonzero momentum matrix element is p_z. Its value [$p_z = 1.7 \times 10^{-20}$ g erg$^{1/2}$] has been taken from Ref. 7. The value of $m_{\parallel}$ ($m_{\parallel} = 1.12m$) has been chosen

TABLE II. Parameters used to fit the absorption coefficient of n-type GaP.

Parameter	Our value	Value from the literature
	Band parameters	
$m_\perp$	$0.254m$	$0.275m$, $0.235m$,[a] $0.25m$[b]
$m_\parallel$	$1.12m$	$0.75m-1.25m$[c]
p_z	1.7×10^{-20} (g erg)$^{1/2}$	$1.6\times10^{-20}-1.9\times10^{-20}$ (g erg)$^{1/2}$[c]
δ	0.357 ± 0.002 eV	0.3 eV[d]–0.355 eV[e]
δ_L	0.09 ± 0.01 eV	0.09 eV[f]
	Donor parameters GaP:S	
E_I	0.106 eV	0.107 ± 0.001 eV[g] 0.107 ± 0.002 eV[h] 0.105 ± 0.005 eV[i]
a	8.5 ± 1 Å	6 Å[j]
b	4 ± 0.5 Å	
b/a	2.1	2.08 ± 2.22[k]
	Donor parameters GaP:Te	
E_I	0.093 eV	0.093 ± 0.001 eV[g]
a	9.5 ± 1 Å	7 Å[j]
b	4.5 ± 0.5 Å	
b/a	2.1	2.08–2.22[k]

[a]Excited donor states magnetospectroscopy, Ref. 8.
[b]Cyclotron resonance, Ref. 6.
[c]Fit of the position of the excited donor states, Ref. 7.
[d]Donor-to-X_3 absorption, Ref. 2.
[e]Absorption to a resonant state, Ref. 3.
[f]Pseudopotential calculations, Ref. 16.
[g]Infrared absorption, Ref. 12.
[h]Luminescence "two-electron transitions," Ref. 9.
[i]Result of the conductivity-versus-temperature measurements on the less-doped sample.
[j]If we treat the E_I as a rydberg, the Bohr radius thus obtained is 6 Å (GaP:S) and 7 Å (GaP:Te).
[k]Reference 7.

to assure the correct position of the first band minimum [$k_0\sim0.1(2\pi/a_0)$] in accordance with Ref. 7. The intensity of the band (b) + (c) + (d) measured at different energies shows a linear variation with concentration (Fig. 4).

The absorption of process (d) has not been previously reported in GaP. Our assignment can be supported by several arguments. The position of the onset agrees with the predicted position of the L minimum obtained in the pseudopotential calculations of Chelikovsky and Cohen.[16] The absorption coefficient of (d) (Fig. 3) seems to decrease more slowly than that of (b), a fact which indicates the presence of indirect transitions. An analogous absorption has been reported in Si,[17] and its maximal cross section is comparable to that found here for process (d).

Within the accuracy of our analysis there is no effect of concentration on the photoionization threshold (which corresponds to a gap $\delta=357\pm2$ meV between the X_1 and X_3 bands). This observation seems *a priori* in contradiction to the results of Galtier *et al.*,[10] where the existence of clustering effects has been demonstrated. It is known that the ground state of an electron in such a pair is lower than the ground state of a single donor. One could then expect a shift of the photoionization threshold with increasing concentration. This is not the case. The pair of neutral donors can be treated approximatively as a H_2 molecule with corresponding distant nuclei. After the absorption of light the electron is emitted to the band and the charged cluster which remains is similar to the H_2^+ ion. The energy of absorbed light with respect to E_I is shown in Fig. 5. It is shown that the energies required for the photoionization of a pair [$E(H_2)-E(H_2^+)$] and of an isolated impurity (E_I) are similar for distances between nuclei greater than five to six Bohr radii, which are like those found in our samples. In that case any differences in the photoionization curves are difficult to see.

B. The resonant state

We expect that the quality of the fit of the photoionization part of the band allows us to get reliable results for the transition from the ground donor state to the resonant state (Fig. 6). This contribution is obtained by subtracting the calculated contribution of processes (a) and (b) from the experimental data. For a given impurity, the energy at the peak position is the same for all samples within 0.5 meV and the former considerations on the photoionization threshold do not apply here because transition (c) occurs between localized states. We obtain a noticeable asymmetry of the line for all samples.

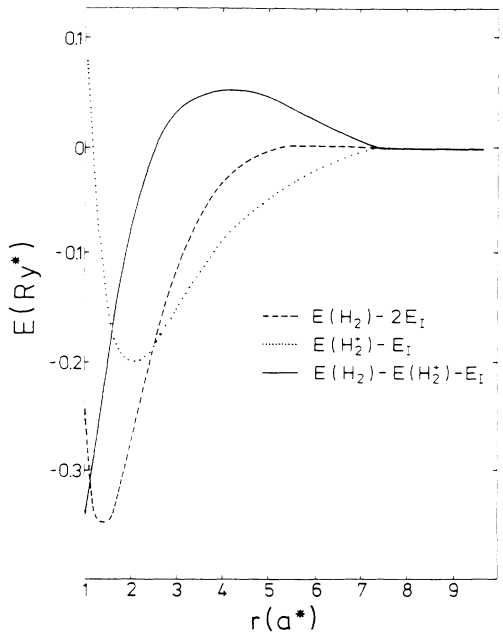

FIG. 5. Energies (in units of the effective Rydberg Ry*) of the H_2 molecule (dashed line), the H_2^+ ion (dotted line), and their difference (solid line) as a function of the distance between nuclei (in units of the effective Bohr radius a^*).

It is worth discussing whether or not this asymmetry is due to the procedure used to extract information about this transition. In fact, an alternative way to deal with it is to assume a symmetrical line shape obtained with a mirror image of the low-energy side with respect to the maximum energy of this transition. In that case, the integrated intensity of the total curve increases more rapidly than the donor concentration, which is difficult to explain. In addition, the subtraction of such a line from the experimental spectra gives a photoionization part which begins with a noticeable tail even for the smallest concentrations, which is in contradiction with the observations of Thomas *et al.*[18]

On the other hand, the asymmetry is expected with the present model [Eq. (9)], a fact related to the Fano effect.[19] Technically, it is possible to fit these curves to an asymmetric Lorentzian line, with a width decreasing linearly as a function of the energy. Indeed, for a Coulombic potential $U(\mathbf{r})$, it can be demonstrated that $\Gamma(E)$ [Eq. (10)] is a decreasing function of the energy and $R(E)$ is negative. This means that the distance between the resonant peak and the onset of the band transitions is smaller than the binding energy of the resonant state.

The energy separation between the peak of transition (c) and the onset of transition (b) requires separate consideration. It amounts to 10 ± 2 meV for all the samples. The resonant state has been assigned previously as $2p'$ in Ref. 3. The symmetry arguments allow for both s' and p' states. The examination of formula (9) indicates that the absorption is proportional to $|\langle\psi_1(\mathbf{r})|\mathbf{p}|\phi_2^0(\mathbf{r})\rangle|^2$. For relatively shallow states, when the wave function can be assumed to be a product of the envelope function times the Bloch function of the band, we get

$$|\langle\psi_1(\mathbf{r})|\mathbf{p}|\phi_2^0(\mathbf{r})\rangle|^2 = p_z^2\left|\int d^3r\, F_1^{0*}(\mathbf{r})F_2^0(\mathbf{r})\right|^2, \quad (12)$$

where $F_2^0(\mathbf{r})$ is the envelope of the localized part $\phi_2^0(\mathbf{r})$ of the resonant-state wave function. This matrix element should vanish when the resonant state is p type and is

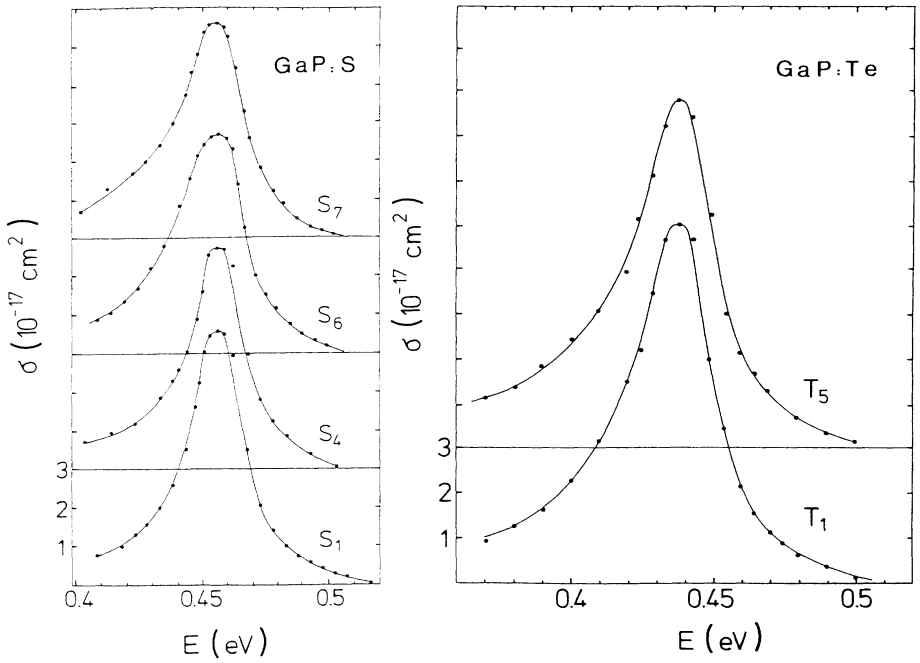

FIG. 6. The transition from a ground state of a donor to a resonant state for different samples GaP:S and GaP:Te. The numbers on the horizontal scale are for the S_1 (T_1) samples, and each following curve is displaced by 0.05 eV for clarity. Dots are experimental points; solid line, the asymmetric Lorentzian curve.

largest for the $1s'$ state. The value of the absorption coefficient for the sample S_1 at the maximum of the (c) peak corresponds to $|\int d^3r\, F_1^0(\mathbf{r})F_2^0(\mathbf{r})| = 0.26$. This can lead to the assignment of the resonant state as the $1s'$ state, a fact noticed by Kopylov in the footnotes of Ref. 13. However, in this case the distance between the resonant peak position and the X_3 minimum has to be explained. The effective-mass theory (EMT) locates the $1s'$ state at an energy between 35 and 45 meV below the bottom of the X_3 band. It can be demonstrated in the simple spherical model (see Appendix) that the shift $R(E)$ near the resonance peak position can amount to 25 meV. Thus we obtain the binding energy of the resonant state around 35 meV, which is in reasonable agreement with the predictions of the EMT. In this way the asymmetry of the line, the resonant peak position, and the absorption selection rules are coherently explained.

We believe that the arguments for the identification of the resonant state as $2p'$ are weaker than ours. The mixing of the Bloch functions due to the antisymmetry crystal potential would allow the $1s$-$2p'$ transition but at X this mixing disappears (it is effective only for $\mathbf{k}\neq 0$). This is, however, beyond the limits of the EMT because the wave function of the resonant state should then be constructed with the whole set of Bloch functions $\psi_2(\mathbf{k},\mathbf{r})$ for different $\mathbf{k}$ points. If this is the case, it is not unlikely that the asymmetry of (c) would be due to a much weaker transition to the $1s'$ state, which would lie below the main $1s$-$2p'$ transition and not be resolved.

The resonant absorption line shape seems to depend on the concentration. It decreases, widens, and becomes more asymmetric when the concentration increases, although the increase of the half-width is small compared to the half-width itself. We expect that this change of shape should correspond to the effect of the concentration broadening of the donor ground and resonant states. We did not attempt to deconvolute the joint density of states of these two levels because of too many unknown parameters in Eq. (9).

VI. CONCLUSIONS

The infrared absorption of GaP doped with S and Te has been measured at $T \simeq 80$ K in the range of 0.25–1.4 eV. The different components of the absorption band have been separated and described by a theoretical model which uses the realistic parameters for the band structure and the donor states. The line shape of the transition to the resonant state has been extracted and appears to be asymmetric. The possible sources of the asymmetry have been discussed. The symmetry properties of X_1 and X_3 require that the resonant state which is seen in absorption is s type, a fact which is *a priori* not consistent with the energy separation between the peak position and the onset of the photoionization transitions, but can be explained by resonance effects. The influence of the neutral-donor concentration of the absorption data has been investigated. It is shown that the photoionization part is not influenced by any pairing effects. There is a small increase in the width of the resonant-state line due to the broadening of the ground and/or resonant donor states with increasing neutral-donor concentration.

ACKNOWLEDGMENTS

The authors wish to thank Professor M. Altarelli for very helpful discussions. One of the authors (E.G.) is greatly indebted to Professor M. Grynberg for his reading of the manuscript and valuable remarks. The Service National des Champs Intenses is "Laboratoire associé à l'Université Scientifique, Techologique et Médicale de Grenoble".

APPENDIX

The shift $R(E)$ and the width $\Gamma(E)$ [Eq. (10)] can be evaluated in a simple model. Let us assume that the impurity potential is Coulombic, the X_1 band is spherical with the effective mass m^* and the $1s'$ state has the form

$$F_2^0(\mathbf{r}) = \frac{\alpha^{3/2}}{\sqrt{\pi}} e^{-\alpha r} .$$

The coupling term (11) is then given by

$$V(\mathbf{k}) = -\frac{4\pi e^2}{\epsilon\sqrt{\pi}} \frac{\alpha^{3/2}}{\sqrt{v}} \frac{1}{\alpha^2+k^2} \frac{1}{\Omega} \int_\Omega u_1(\mathbf{k},\mathbf{r}) u_2^*(\mathbf{k}_X,\mathbf{r}) d^3r .$$

The integral

$$M(\mathbf{k}) = \frac{1}{\Omega} \int_\Omega d^3r\, u_1(\mathbf{k},\mathbf{r}) u_2^*(\mathbf{k}_X,\mathbf{r})$$

has been calculated by means of the local-pseudopotential method[20] along three different directions, $(0,0,\xi)$, $(\xi,\xi,1)$, and $(\xi,\xi,1-\xi)$, around the X point. A typical variation of $M(\mathbf{k})$ is shown in Fig. 7 as a function of the energy. The mean value of M over a surface of constant energy $E_{X_1}(\mathbf{k}) = 165$ meV (the resonance energy) is 0.57. The region on this surface where $M(\mathbf{k}) < 0.3$ is less than 25% of the total surface. If, in a first approximation, we treat $M(\mathbf{k})$ as a constant M, then

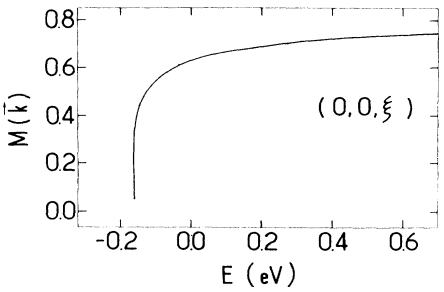

FIG. 7. Typical variation of the matrix element $M(\mathbf{k})$ along the direction $(0,0,\xi)$ as a function of energy. The calculation has been performed with the parameters obtained from the empirical pseudopotential method (Ref. 20) and the origin of the $\mathbf{k}$ vector taken at the Γ point of the Brillouin zone.

$$R(E)=\frac{-\alpha^3}{(2\pi)^3}M^2\left[\frac{4\pi e^2}{\epsilon}\right]^2\frac{4m^*}{\hbar^2}\times\left[\frac{2\pi}{4\alpha(\alpha^2+\beta^2)}+\frac{2\pi\alpha}{2(\alpha^2+\beta^2)^2}\right]$$

with

$$\beta^2=\frac{2mE}{\hbar^2}\ ,$$

$$\Gamma(E)=\frac{\alpha^3}{(2\pi)^3}M^2\left[\frac{4\pi e^2}{\epsilon}\right]^2 2\pi\left[\frac{\hbar^2}{2m^*}\right]^{1/2}\frac{\sqrt{E}}{\left[\frac{\hbar^2\alpha^2}{2m^*}+E\right]^2}\ .$$

$R(E)$ and $\Gamma(E)$ do not depend much on m^*, which justifies such an approach. However, they increase significantly when the mean radius of the $1s'$ state decreases. For $1/\alpha=8-10$ Å the shift is found to be in the range -20 to -30 meV. A simple estimation from the isotropic effective-mass theory gives $1/\alpha\simeq 15$ Å. The real wave function is anisotropic with the radius $1/\alpha$ smaller in the z direction (e.g., 9 Å), than in x or y. In that direction M is larger than the mean value and can reach 0.65. The largest contribution to the total shift and width comes then from the region of the surface $E_{X_1}(\mathbf{k})=165$ meV near the z axis. In this region, for small values of $1/\alpha$ the ratio $R(E)/\Gamma(E)$ is equal to -2.0 ± 0.2. Of course, the total shift $R(E)$ and width $\Gamma(E)$ have to be weighted by the different values of M and $1/\alpha$. But, since the ratio $R(E)/\Gamma(E)$ is nearly constant, we can expect that the observed shift is twice as large as the experimentally observed half-width (12.5 meV for the lowest doped sample S_1), which corresponds for $R(E)$ to a value around -25 meV. This gives 35 meV for the binding energy of the $1s'$, state which is in reasonable agreement with the predictions of the EMT (35–45 meV).

[1]W. G. Spitzer, M. Gershenzon, C. J. Frosch, and D. F. Gibbs, J. Phys. Chem. Solids **11**, 339 (1959).

[2]A. N. Pikhtin and D. A. Yaskov, Phys. Status Solidi **34**, 815 (1969).

[3]A. Onton, Phys. Rev. B **4**, 4449 (1971).

[4]P. Lawaetz, Solid State Commun. **16**, 65 (1975).

[5]T. Morgan, Phys. Rev. Lett. **12**, 819 (1968).

[6]N. Miura, G. Kido, M. Suekane, and S. Chikazumi, in Proceedings of the 16th ICPS, Montpellier, France, edited by M. Averons [Physica **117&118B/C**, 66 (1983)].

[7]Y. C. Chang and T. C. McGill, Solid State Commun. **33**, 1035 (1980).

[8]A. C. Carter, P. J. Dean, M. S. Skolnick, and R. A. Stradling, J. Phys. C **10**, 5111 (1977).

[9]R. A. Onton and R. C. Taylor, Phys. Rev. B **6**, 2587 (1970).

[10]P. Galtier, G. Martinez, P. Lambert, and M. Gauneau, Phys. Rev. B **33**, 6909 (1986).

[11]W. L. Bond, J. Appl. Phys. **5**, 1674 (1965).

[12]A. A. Kopylov and A. N. Pikhtin, Phys. Tech. Semicond. **5**, 867 (1977), in Russian.

[13]A. A. Kopylov, Solid State Commun. **1**, 1 (1985).

[14]Y. C. Chang and T. C. McGill, Phys. Rev. B **10**, 5779 (1981).

[15]F. Bassani and G. Pastori Paraviccini, in *Electron States and Optical Transitions in Solids,* edited by R.A. Ballinger (Pergamon, New York, 1975).

[16]J. R. Chelikovsky and M. L. Cohen, Phys. Rev. B **12**, 556 (1975).

[17]W. Spitzer and H. Y. Fan, Phys. Rev. **2**, 268 (1957).

[18]G. A. Thomas *et al.*, Phys. Rev. B **10**, 5472 (1981).

[19]U. Fano, Phys. Rev. **6**, 1966 (1961).

[20]J. Chelikovsky, D. J. Chadi, and M. L. Cohen, Phys. Rev. B **8**, 2786 (1973).